

TEMPORAL AND SPATIAL VARIABILITY OF DAILY INTENSITY RAINFALL AND THEIR RELATION WITH SURFACE ATMOSPHERIC CIRCULATION IN SOUTHEASTERN SOUTH AMERICA

Federico A. Robledo * ^{1,2} and Olga C. Penalba¹

¹Departamento de Ciencias de la Atmósfera y los Océanos, FCEN, UBA, Buenos Aires

²Consejo Nacional de investigaciones Científicas y Tecnológicas (CONICET), Buenos Aires,

1. INTRODUCTION

Groisman et al. (2005) have found a systematic increase in very heavy daily precipitation in the subtropical part of Brazil since the 1940s. Haycock et al. (2005) found changes in the annual extreme rainfall indices, examining daily rainfall data from 1961 to 2000 in twelve stations in South America. Pscheidt et al. (2006) found extensive areas in southern Brazil where the frequency of extreme precipitation events significantly increased in November of El Niño years and decreased during the La Niña years. Re et al. (2006) analyzed the temporal variability of frequency of daily extreme precipitation events (greater than 80 mm/day and 100mm/day), finding positive trends in central and eastern Argentina. Penalba and Robledo (2008) analyzed temporal variability of the extreme daily precipitation events from 1961 to 2000. They observed positive and significant trends during autumn season in south of Brazil and east of Argentina. However, they observed negative trends during winter season in central-east of Argentina. During the last years, many authors discussed the changes of the low-level circulation, both at regional and global scales.

For example, at regional scale, some results show a southward shift of the South Atlantic high (SAH) (Camilloni, 1999; Camilloni et al. 2005), a displacement to the south of the regional atmospheric circulation over southeastern South America (Barros et al. 2000) and an enhancement of the easterly winds during the summer months over the Río de la Plata estuary (Simionato et al. 2005). These regional trends seem to be part of a more general hemispheric behaviour. Gibson (1992) showed a poleward shift of 3° of latitude on the maximum wind at 500 hPa in the 1976-1991 periods. Van Loon et al (1993) calculated the latitude of the zonally averaged subtropical ridge over the Southern Hemisphere, finding a 2° trend over the 1976-1990 periods. The sea level pressure pattern has predominantly positive trends at the 30°-45° latitude band of the Southern Hemisphere, and a trend of more than 2 hPa in the South Atlantic (Gillet et al, 2003). Di Luca and Camillioni (2006) shown that there are three predominant patterns that characterize seasonal sea level pressure fields over an extensive region of the Southern Hemisphere, covering the southern South America and the adjacent oceans, Atlantic and Pacific. They found a summer surface circulation with the South Atlantic and South Pacific highs in their southernmost positions and a winter circulation with the South Atlantic and South Pacific in the northernmost position.

* *Corresponding author address:* Federico A. Robledo. DCAO. Facultad de Ciencias Exactas y Naturales. Universidad de Buenos Aires - Argentina Intendente Güiraldes 2160, 2º piso - Ciudad Universitaria- C1428EGA – e-mail: frobledo@at.fcen.uba.ar

The objective of this work is firstly to analyze the seasonal patterns of the daily intensity of extreme rainfall (DIER) and their temporal variability. In addition, an analysis of the surface atmospheric circulation in the South Atlantic Ocean will be improved to evaluate his influences in the observed changes in the intensity of extreme rainfall.

2. DATA AND METHODOLOGY

To perform the analysis two data base in the period 1978-2006 were used.

* Monthly mean 1000 hPa geopotential height fields corresponding to NCEP/NCAR reanalysis over an area between 20°S-45°S and 67,5°W-0°W.

* High quality daily rainfall for 35 surface stations (Figure 1).

The analyzed period was conditioned by the reanalysis data. They are more representative of real data over the oceanic areas only after 1978 when satellite data began to be fully used (Sturaro 2003).

At this work a seasonal analysis is performed, evaluating two different indices: a) seasonal mean 1000 hPa geopotential height fields (here after: seasonal 1000hPa index); and b) seasonal daily intensity of extreme rainfall index (seasonal DIER index).

The monthly mean of daily intensity of extreme rainfall (DIER) is the quotient between monthly accumulated extreme rainfall (AE) and the number of days with extreme precipitation in one month (PE).(See Equation 1)

$$DIER_{i,j} = \frac{AE_{i,j}}{PE_{i,j}}$$

Equation 1. Daily intensity of extreme rainfall index (DIER_{i,j}), where *i* represent months (1 to 12) and *j* represent the years (from 1962 to 2005).

In this work, we considered an extreme precipitation day when rainfall it is greater than mean 75th daily percentile for the period 1961-2000 (Penalba and Robledo 2008). The seasonal DIER index was calculated averaging the monthly DIER.

T-mode Varimax Rotated Principal Components Analysis was used to identify the seasonal dominant patterns of the two indices.

3. RESULTS

3.1. Spatial pattern of seasonal DIER index

Figure 2 shows the fourth predominant patterns of seasonal DIER index, explaining almost 67.8% of the total variance. The first principal component (PC1) explains 25% of the total variance and represents the summer DIER pattern (Penalba and Robledo 2008). PC1 resembled the extreme precipitation equatorward 30° S in the north of Argentina. In the seasonal contribution analysis of PC1, the summer explains 44.7%, spring and autumn: 27.4% and 22.8% (Table 1).

The second principal component (PC2) explains 18% of the total variance and represents the winter DIER pattern (Penalba and Robledo 2008) (Figure 2). PC2 resembled a maximum precipitation eastward 60°W in east Argentina, south Brazil and Uruguay. In the seasonal contribution analysis of PC2, the winter explain

57.2%, and spring and autumn: 19.2% and 18.2% respectively (Table 1).

PC3 and PC4 explain 13.8% and 9.6 % of the total variance respectively and have two opposite center of maximum and minimum (Figure 2). These patterns are not resembled any mean season field of DIER. In addition, when the seasonal contribution analysis is performed, none season has a preferential explanation (Table 1).

3.2. Spatial pattern of seasonal 1000hPa index

Figure 3 shows the fourth PCs of seasonal 1000hPa index, which explained almost 96% of the total variance. The first pattern (PC1) explains 54% of the total variance and represents the summer surface circulation (Di Luca and Camilioni, 2006). In the seasonal contribution analysis of PC1, the summer explains 38.1% and spring 31.7% (Table 2). This pattern is similar to the summer mean surface circulation and has the South Atlantic highs in their southernmost position.

PC2 explains 35% of the total variance and represents the winter circulation in northernmost position (Di Luca and Camilioni, 2006). In the seasonal contribution analysis of PC2, winter and autumn seasons explain 50.9% and 24% respectively (Table 2).

PC3 and PC4 explain 5.3% and 2.1 % of the total variance respectively (Figure 3) and have an important seasonal contribution to the autumn circulation (Table 2).

3.3. Spatial pattern of autumn 1000hPa

In order to analyze the atmospheric circulation associated with seasonal extreme intensity, the patterns with low explained total variance were analyzed in more detail, which are associated with autumn season (Table 2). To analyze only this behavior, principal component analysis was applied to the autumn 1000hPa index

Figure 4 shows the third PCs of autumn 1000hPa patterns, which explained almost 92% of the total variance. The first pattern (PC1) explains 36% of the variance and represents the mean autumn surface circulation. This pattern has the South Atlantic highs in an intermediate position between summer and winter circulation (Figure 4). PC2 and PC3 explain 32% and 24% of the total variance respectively. Both patterns have the South Atlantic High shift to the east respect the PC1. Nevertheless, PC3 pattern resembled the South Atlantic high southward (35°-40°S) respect the PC2 (30°-35°S) (Figure 4). PC2 suggests a northeast surface wind in the northeast of Argentina, while PC3 represent a southwest circulation.

The temporal variability of the factor loading of each PCs is analyzed (Figure 5). During the years that the factor loadings 1 (FL1) are low the FL2 and/or FL3 show high values. This could be associated with a mean autumn surface circulation debilitated and with a PC2 and PC3 patterns stronger. The linear correlations between FL1-FL2 (Figure 5, above) and FL1-FL3 (center) are negative and significant, -0.54 and -0.48 respectively. Nevertheless, FL2 and FL3 are out of phase (Figure 5, below). The linear correlation of this FLs is negative (-0.33, significant at 10%), suggesting that the PC2 and

PC3 can be alternate as long as the mean surface circulation of autumn is perturbed. When the mean surface field is perturbed, the South Atlantic high shifts to the east and have a north-south oscillation around 30°S. This spatial variability is not characteristic of all seasons. Only during autumn season the north-south alternate pattern is predominant, when the South Atlantic High shifts to the east. The north-south oscillation is accompanied by different atmospheric circulation over the continental.

3.4. Relation between DIER and 1000hPa during autumn

Previous to the coupled analysis, the temporal variability of the autumn DIER patterns is analyzed. During this season, factor loading of PC3 and PC4 are out phase, with a negative and significant (5%) correlation -0.38 (Figure 6). To perform the autumn relationship between DIER and 1000hPa indices, the temporal variability of the PCs is analyzed.

Figure 7 shows the FL2 of autumn 1000hPa (FL2HGT) and FL3 of autumn DIER (DIERFL3) and FL4 of autumn DIER (DIERFL4). The linear correlation between FL2HGT and DIERFL4 is positive (0.22, not significant), showing coupled variability between PC2 of autumn 1000hPa and PC4 of autumn DIER. Between 1989 and 1994 FL2HGT, DIERFL3 and DIERFL4 shows an important inter-annual variations.

In the figure 7, the black arrows indicate the different phases of warm sea surface temperature of El Niño/Southern Oscillation (ENSO). During El Niño years the relation between FL2HGT and DIERFL4 increases (0.42,

without being significant). The linear correlations between FL2HGT and DIERFL3 are negative, suggesting that the PC2 1000hPa pattern does not have direct influence in the DIER4 rainfall pattern.

Figure 8 shows the scattering between FL2HGT and DIERFL4 for the different phases of ENSO. The Niña years (blue triangles) show a lower factor loading coefficient (0.18) of DIERFL4 respect the El Niño years (blue squares) coefficients (0.6). Nevertheless, autumn surface circulation (FL2HGT coefficient) does not have a clear difference signal during the opposite phases of ENSO.

4. CONCLUSION

The objective of this work is firstly to analyze the seasonal patterns of the daily intensity of extreme rainfall (DIER) and their temporal variability. In addition, an analysis of the surface atmospheric circulation in the South Atlantic Ocean will be improved to evaluate his influences in the observed changes in the intensity of extreme rainfall

To perform the analysis two data base in the period 1978-2006 were used: Monthly mean 1000 hPa geopotential height fields over an area between 20°S-45°S and 67,5°W-0°W and high quality daily rainfall for 35 surface stations.

These studies suggest that when the mean surface circulation field is perturbed, the South Atlantic high shifts to the east and have a north-south oscillation around 30°S. This oscillation is not characteristic of all seasons, being predominant during autumn. In addition, the north-south oscillation is accompanied by

different surface circulation structures over the continent.

In the ENSO phases, different surface structures alternate, especially in autumn. During El Niño years there are two predominant patterns: the South Atlantic High shifted to the east with a south-north oscillation and a local circulation generated over south of Brazil and Uruguay (Figure 4, PC2). This secondary pattern has a predominant direction northeast to southwest in the northeast of Argentina; this surface pattern is associated with enhancement of the autumn extreme daily rainfall (Figure 2 PC4 DIER). During La Niña years the local surface circulation is not associated with more extreme daily rainfall in the northeast of Argentina during autumn.

Acknowledgements

Support for carrying out this work was provided by the following Grants: University of Buenos Aires X170, CLARIS La Plata Basin Project (European Commission Project) and PICT05 38273-ANPCYT.

5. REFERENCES

Barros V.; M.E. Castañeda and M.Doyle. 2000: Recent precipitation trends in Southern South America to the East of the Andes: an indication of a mode of climatic variability. In: Smolka P, Wolkheimer W (eds) *Southern Hemisphere Paleo and Neoclimates Concepts, Methods, Problems*. Springer, Berlin, 187-206.

Camilloni, I. 1999: Temporal variability of the Buenos Aires' urban heat island intensity. *International Conference on Urban Climatology ICUC'99*, Sydney Australia.

Camilloni, I.; V. Barros and A. Di Luca. 2005: Trends in the position of the South Atlantic high and its representation by Global Climate Models: impacts over the Río de la Plata estuary and adjacent ocean (in Spanish). *Preprints of IX Congreso Argentino de Meteorología*. Buenos Aires, Argentina.

Di Luca, A.; Camilloni, I. and V. Barros, 2006: Sea-Level pressure patterns in South America and adjacent oceans in the IPCCAR4 models. *Proceedings of 8 ICSHMO*, Foz do Iguaçu, Brazil, April 24-28, 2006, INPE, p. 235-243

Gibson, T. 1992: An observed poleward shift of the Southern Hemisphere Subtropical wind maximum: A greenhouse symptom?. *Int. J of Climatol* **12**, 637-640

Gillett, N; F. Zwiers, A. Weaver and P. Stott. 2003: Detection of human influence on sea-level pressure. *Nature* **422**, 292-294.

Penalba, O. and Robledo, F., 2008: Spatial and temporal variability of the frequency of extreme daily rainfall regime in the La Plata Basin during the 20th century. *Climatic Change*. In press

Simionato, C.; C.Vera and F. Siegmund. 2005: Surface wind variability on seasonal and interannual scales over Río de la Plata. *J. of Coastal Research* **21**, 770-783.

Van Loon H, J. Kidson and A. Mullan. 1993: Decadal variation of the annual cycle in the Australian Data Sets. *J. of Climate* **6**, 1227-1231.

6 ILLUSTRATIONS AND TABLES

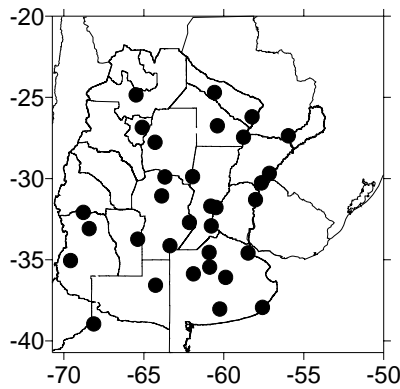


Figure 1. Geographic distribution of the stations used in the study.

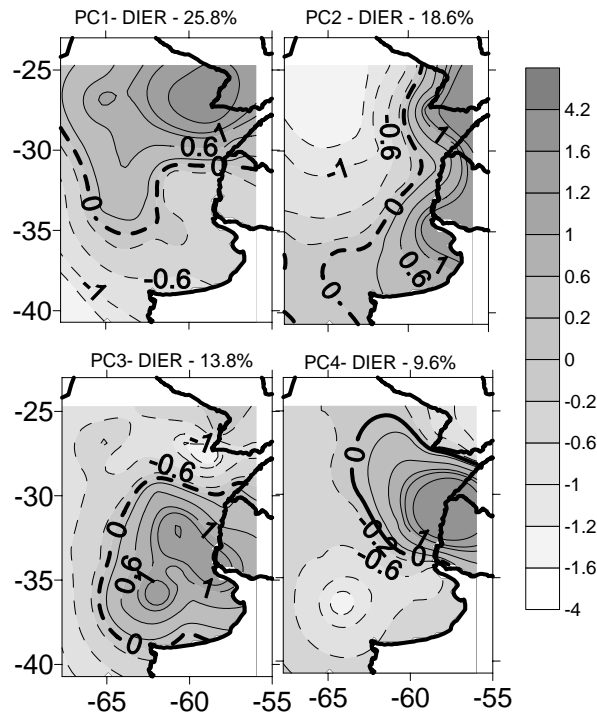


Figure 2. Principal Components of the daily intensity of extreme rainfall (DIER index, rainfall greater than mean 75th daily percentile).

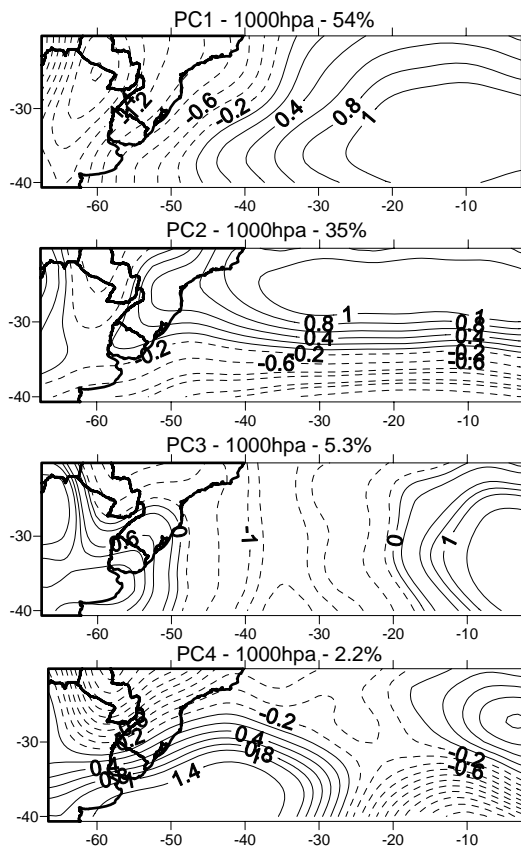


Figure 3. Principal Components of the 1000hPa index

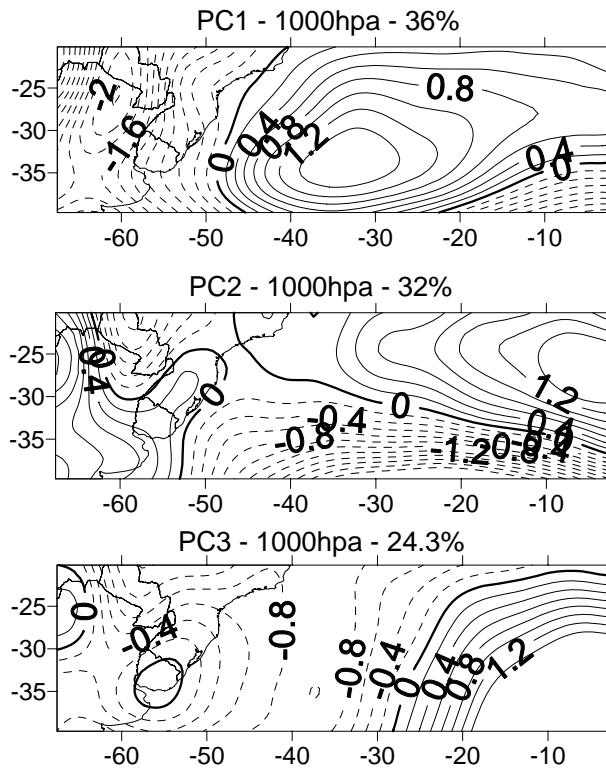


Figure 4. Principal Components of autumn 1000hPa index.

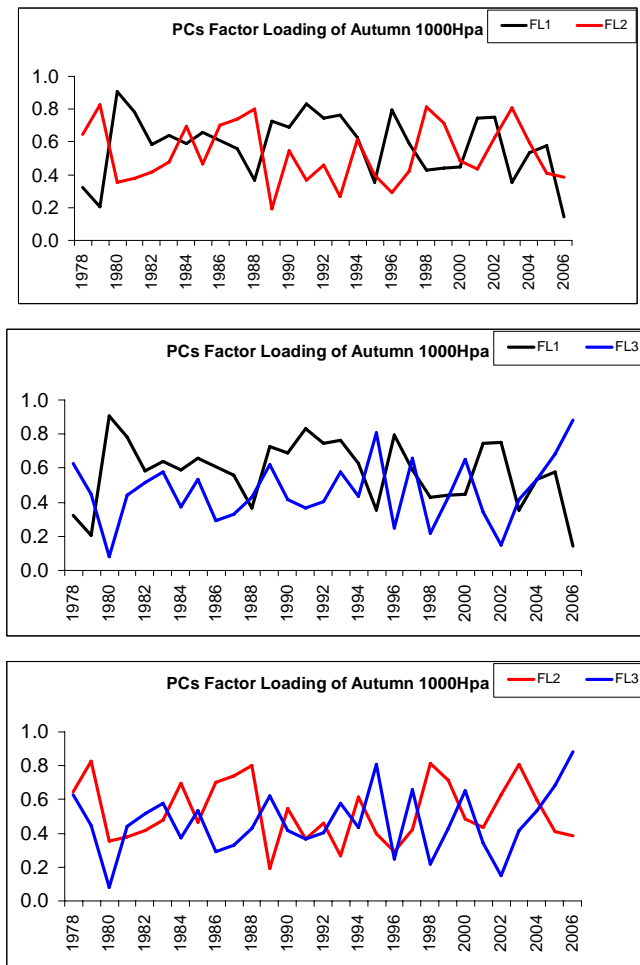


Figure 5. Factor Loading of autumn 1000hPa index. Above: FL1 (black) and FL2 (Red). Center: FL1 (black) and FL3 (Blue). Below: FL2 (Red) and FL2 (Blue).

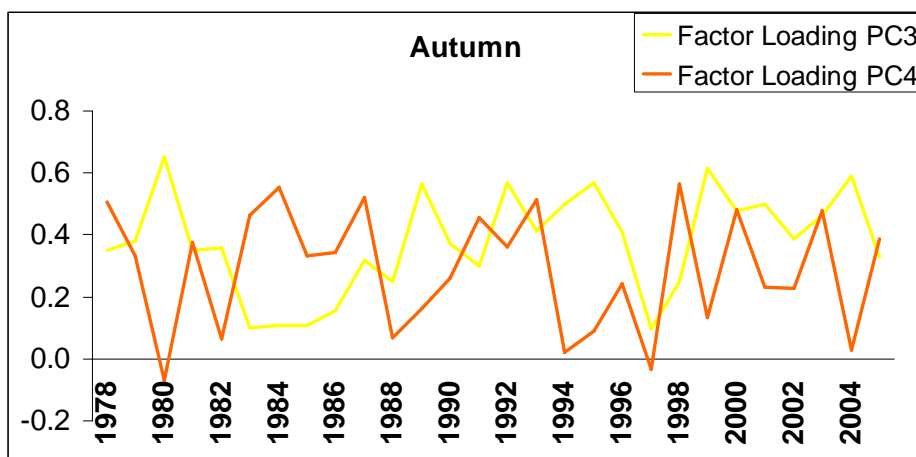


Figure 6. Factor Loading of autumn for DIER PC3 (yellow) and PC4 (orange)

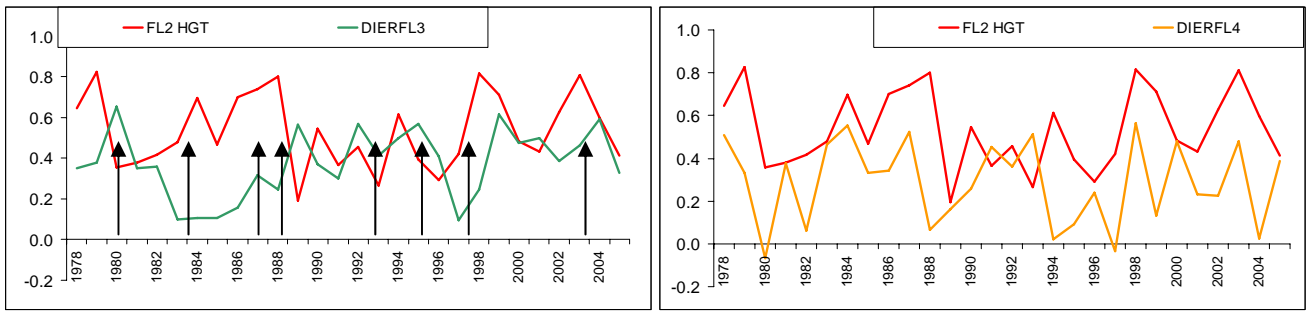


Figure 7. Factor Loading of 1000hPa autumn (red) and: left: DIERFL3 (green). Right: DIERFL4 (orange). The black arrows indicate the different phases of warm sea surface temperature of El Niño/Southern Oscillation

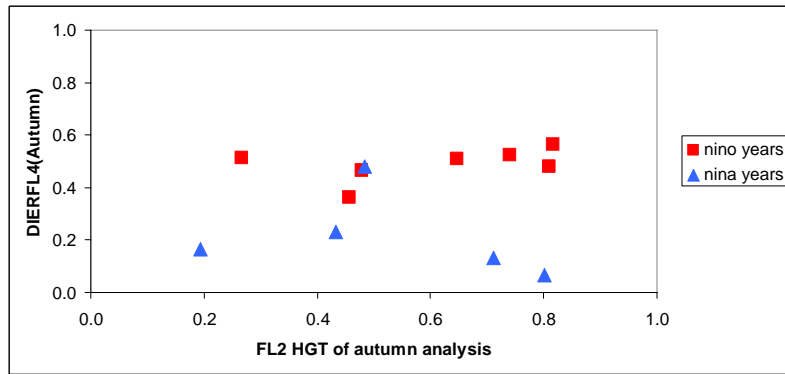


Figure 8. Scattering figure between DIERFL4 and FL2HGT, for the different phases of ENSO: El Niño year (red squares) and La Niña year (blue triangle).

	PC1	PC2	PC3	PC4
Summer	44,7	5,4	20,0	7,9
Winter	5,1	57,2	14,4	35,3
Autumn	22,8	18,2	30,3	31,5
Spring	27,4	19,2	35,3	25,2
Total	100	100	100	100

Table 1. Seasonal contribution (%) to the total variance of the first PCs of seasonal DIER index.

	PC1	PC2	PC3	PC4
Summer	38,1	9,2	11,3	4,2
Winter	10,1	50,9	9,1	19,4
Autumn	20,1	24,0	63,3	42,5
Spring	31,7	15,9	16,4	33,8
Total	100	100	100	100

Table 2. Seasonal contribution (%) to the total variance of the first PCs of seasonal 1000hPa index.